Influence of Surrounding Conditions and Fuel Size on the Gasification Rate of Biomass Char in a Fluidized Bed

Influence of Surrounding Conditions and Fuel Size on the Gasification Rate of Biomass Char in a Fluidized Bed

Louise Lundberg[a*], Placid A. Tchoffor[b], David Pallarès[a], Robert Johansson[a], Henrik Thunman[a], Kent Davidsson[b]

[a]*Department of Energy and Environment, Chalmers University of Technology, SE-412 96 Göteborg, Sweden*

[b]*SP Technical Research Institute of Sweden, SE-501 15 Borås, Sweden*

**Telephone: +46 31 772 1438, E-mail: louise.lundberg@chalmers.se*

Abstract

While the operational conditions of a fluidized bed are known to influence the fuel axial mixing, the effect of the resulting axial location of the fuel particles on the char gasification rate remains unexplored. In this work, a laboratory-scale bubbling fluidized bed was used to investigate how the gasification rate of biomass char was influenced by the fuel axial location (during pyrolysis and char gasification), the pyrolysis atmosphere, the fuel size, and the fuel concentration. When pyrolysis at the bed surface was followed by char gasification inside the dense bed the char gasification rate was up to 2-fold lower than the other combinations of the fuel axial location, which held similar rates. Cooling the char after pyrolysis decreased the char gasification rate in all cases studied. The gasification rate increased when the fuel particle size was decreased, and its dependence on the degree of char conversion was also affected. Thus, the operational conditions of a fluidized bed reactor, through modified fuel axial mixing, can influence the char gasification rate. Furthermore, experimental determination of reactivity data in laboratory-scale systems must account for the axial location of the fuel at the desired end-scale, using similar fuel particle sizes.

Keywords: fluidized bed, char gasification, biomass char, fuel segregation, char kinetics

Nomenclature

C_b	accuracy in carbon balance (-)
HR	heating rate (ºC/s)
E_a	activation energy (J/mole)
$f(X)$	structural model (-)
k_0	pre-exponential factor ($s^{-1}bar^{-n}$)
m_0	initial mass of dry ash-free fuel (kg)
M_C	molar mass of carbon (kg/mole)
m_C	mass of carbon in fuel (kg)
$m_{C,C}$	mass of carbon measured during char combustion (kg)
$m_{C,G}$	mass of carbon measured during char gasification (kg)
$m_{ch,CG}$	mass of ash-free char in basket after char gasification (kg)
$m_{ch,f}$	mass of ash-free char fines in reactor after pyrolysis (kg)
$m_{ch,P}$	mass of ash-free char in basket after pyrolysis (kg)
$\dot{m}_{C,out}$	mass flow of carbon leaving the reactor (kg/s)
n	steam dependency (-)
$\dot{n}_{N_2}$	flow of N_2 through reactor (mole/s)
P_{reac}	partial pressure of reactant (bar)
R	gas constant (J/mol/K)
R_{ch}	char reactivity (s^{-1})
R_m	char gasification rate (s^{-1})
t	time (s)
T	temperature (K)
T_F	fuel temperature (K)
$T_{F,0}$	initial fuel temperature (K)
u_{mf}	minimum fluidization velocity (m/s)
X	degree of char conversion (-)
Y_i	molar fraction of i (mole/mole)
Y_{ch}	char yield (kg/kg daf fuel)

Acronyms

BC	boundary conditions
BET	Brunauer–Emmett–Teller
BS	on the bed surface
CG	char gasification
$DFBG$	dual fluidized bed gasification
F	free
FB	fluidized bed
HA	high accuracy
IB	inside the dense bed
LA	low accuracy
P	pyrolysis
SEM	scanning electron microscope
SNG	substitute natural gas
TGA	thermogravimetric analysis
WC	wood chips
WP	wood pellets

1 Introduction

Fluidized bed (FB) biomass gasification is a promising technology for transforming lignocellulosic materials into a raw gas that can be further upgraded to transportation fuels, such as methanol, dimethyl ether, Fischer-Tropsch diesel, and substitute natural gas (SNG) [1, 2]. The main advantages associated with FB units are relatively good gas-fuel mixing, even temperature distribution, and good flexibility in terms of usable fuels [3, 4]. However, FB units are limited to operating temperatures below 900°C due to the risk of agglomeration and sintering of the bed material [3, 4]. Two major FB techniques can be used for biomass gasification: direct gasification, for which the heat demand is met by combusting a fraction of the fuel inside the gasification chamber [2, 5]; and indirect gasification (or dual fluidized bed gasification, DFBG) [1, 5]. In DFBG, unconverted char is transported with the bed material from the gasification chamber to a combustor, and the heat required for gasification is provided by recirculating the hotter bed material from the combustor to the gasifier.

The present work was carried out within the framework of the GoBiGas project [6], which aims to produce SNG on a commercial scale (80–100 MW) using DFBG. Currently, three different gasifier size scales are being used to improve understanding of the processes that occur within a DFBG system: 1) a laboratory-scale bubbling FB gasifier [7]; 2) the 2–4-MW Chalmers gasifier [8]; and 3) a 20-MW demonstration plant operated by Göteborg Energi [6]. A mathematical model of the gasifier of a DFBG system is also being developed [9], with the aim of investigating different design parameters for the optimisation and upscaling of this type of gasifier.

As discussed by Larsson et al. [8], given a specific fuel, the degree of char conversion in the gasification chamber is the main parameter that needs to be controlled for optimisation of the output of a DFBG system. Thus, for the design, up-scaling, and evaluation of a new fuel type, it is crucial to be able to predict the rate of char gasification as accurately as possible. The distinction between char reactivity and char gasification rate, see Fig. 1, should be noted. The char reactivity is a characteristic property of the char, which encompasses the kinetics (the dependency of the temperature and the concentration of the gaseous reactant), as well as structural effects (the change of the char porosity and the total surface area with the degree of conversion of the char particle, X). Furthermore, the char reactivity is also affected by a number of factors such as the ash content and composition [10] and the inhibitory effects of certain gas species [11], see below. Assuming n^{th} order kinetics, the char reactivity can be expressed as:

$$R_{ch} = k_0 e^{-\frac{E_a}{RT}} P_{reac}^{n} f(X) \tag{1}$$

In contrast, the char gasification rate is the apparent rate, which also includes external and internal mass transfer resistances. Thus, while drying and pyrolysis (the two other conversion processes that solid fuel undergoes in a gasifier) are limited by heat transfer, the rate of char gasification is affected by several variables, including the char kinetics, the char structure, diffusional resistances, and the fuel particle size [12, 13] (Fig. 1).

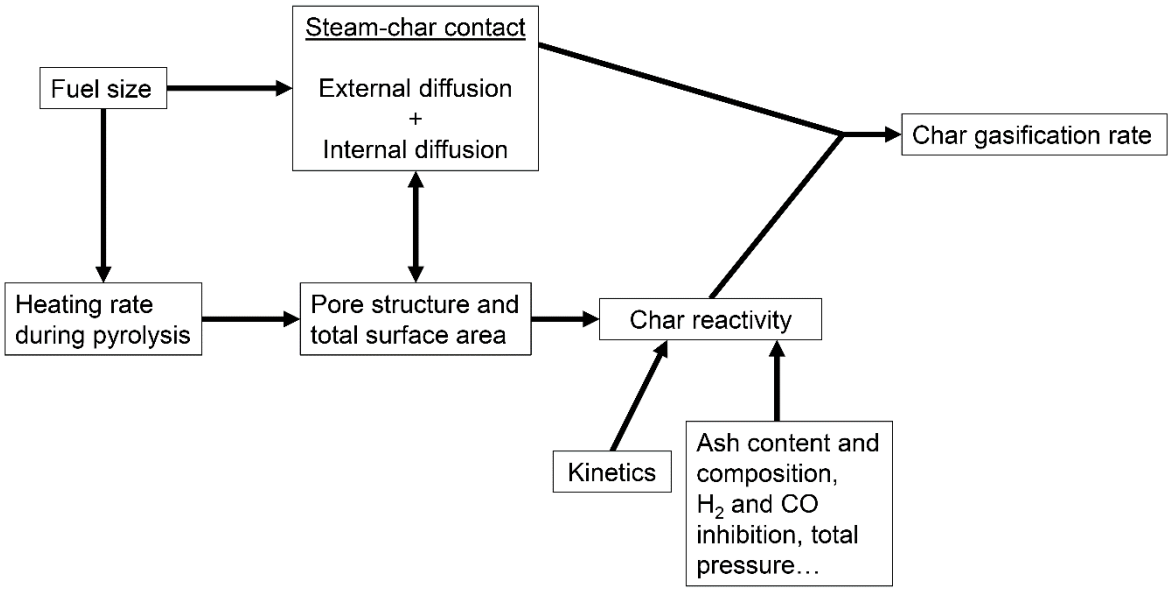

Figure 1. Definitions of the reactivity and the gasification rate used in this work. The figure also shows how different parameters are connected to the char reactivity and the gasification rate.

In order to understand how the degree of char conversion in the gasification chamber of a DFBG system is affected by different parameters, accurate modelling is a valuable tool, in which kinetic and structural parameters of quantitative relevance are key [9]. There is a vast body of literature on char reactivity. Thermogravimetric analysis (TGA) is a standard method used to investigate the reactivity of biomass char at relatively low heating rates [14, 15]. Fluidized bed gasifiers have also been used in several studies aimed at investigating the reactivities of coal char [16-20] and biomass char [13, 18, 21-23]. In addition to determining the char kinetics, these studies have examined how the following factors influence char reactivity: fuel type [16, 18, 20]; surface area and porosity [16, 18]; catalytic effects [18]; time of pyrolysis [16, 19, 20]; total pressure during gasification [19]; and partial pressure of H_2 [19]. The effects of particle size and cooling of the particles prior to char gasification have been studied [13], as well as the inhibitory effects of H_2 and CO [22]. Moreover, char gasification in mixtures of CO_2 and H_2O has received attention [22, 23].

In a review published by Di Blasi [14], the activation energies for steam gasification of biomass are listed as in the range of 143–237 kJ/mol. The large variability in the kinetic parameters of biomass char is mainly due to the differences in ash content and composition of various types of biomass. For example, Ca and K have been observed to have a catalytic effect on char gasification [24-26]. However, in the presence of high concentrations of Si, K can form silicates that eventually deactivate its catalytic effects [27, 28]. Furthermore, sintering of ash can block the char pores [29, 30], which leads to a decrease in char reactivity. In addition to this intrinsic heterogeneity of different types of biomass, the surrounding conditions, including the heating rate and the steam-char contact during pyrolysis and char gasification, have significant impacts on char reactivity by affecting the char structure [7, 14].

Several authors have shown that chars formed at high heating rates are much more (2–3-fold more [14]) reactive than those produced at low heating rates [10, 31-34]. If a low heating rate

is used during pyrolysis, the morphology of the fuel particles remains more or less unchanged, since the outflow of volatile gases is rather slow [31, 35]. The char formed under such conditions consists mainly of micropores [31], and the char yield is relatively high, since repolymerisation can occur during the relatively slow transport of volatiles through the fuel particle [32]. If a high heating rate is used, the volatile yield is much higher, resulting in a rapid outflow of volatile gases and a lower char yield. Furthermore, the particles are more likely to undergo plastic deformation [31]. The char is more porous than that formed using a low heating rate, and mesopores and macropores, which seem to be more reactive than micropores [10, 31], are present to a larger extent [31]. The total surface area is also larger for chars produced at a high heating rate [31]. As seen in Fig. 1, besides affecting the resistance to diffusion of the fuel particle, the fuel size also affects the heating rate and thus the char reactivity itself; smaller particles have higher heating rates, which make them more reactive than larger fuel particles [12].

Another phenomenon that affects char reactivity is that the total surface area and pore volume increase when the char comes into contact with steam [7, 36]. Tchoffor et al. [7] observed that after pyrolysis of wheat straw pellets, the Brunauer–Emmett–Teller (BET) surface area and pore volume of the char were very low, whereas when the char was exposed to steam, the BET surface area and the pore volume increased with the duration of steam exposure. Thus, as seen in Fig. 1, in addition to directly influencing the char gasification rate, the steam-char contact resulting from the external and internal mass transport of steam influences the char reactivity itself by affecting the char structure. While effectiveness factors are sometimes used to model the effects of the diffusional resistances on the gasification rate [15], the effect of the steam-char contact on the char structure and the resulting char reactivity needs to be accounted for by the reactivity model, but is largely unknown.

The heating rate of fuel particles in a fluidized bed is higher when the particles are immersed in the dense bottom region than when they are located on or above the dense bed surface, due to the increased direct contact with the inert bed material. In contrast, the gas mass transfer between the fuel and the bed is lower in the emulsion phase of the dense bed than on the bed surface, due to the blocking effect of the bulk solids. Furthermore, the fluidization velocity influences the axial location of wood pellets in the gasifier of a DFBG system, as observed by Berdugo Vilches et al. [37]. With the aid of a hot-temperature camera probe they found that at low fluidization velocities ($< 3.5 \cdot u_{mf}$), the level of axial fuel segregation was high, with fuel particles being more likely to be located on the surface of the bed. As the fluidization velocity was increased, axial mixing intensified, making it more likely for the fuel particles to become immersed in the dense bed. Increasing the fluidization velocity above $8 \cdot u_{mf}$ had no further effect on the fuel axial mixing. An additional phenomenon that needs to be considered regarding fuel vertical mixing is the formation during pyrolysis of endogenous bubbles, which have been observed to lift fuel particles to the bed surface [38], although it is not clear to what extent this phenomenon prevails as the fluidization velocity is increased. Thus, the conditions under which a fluidized bed is operated can influence the char gasification rate by affecting the fuel mixing and thereby: 1) the external mass diffusion to the fuel particles, which in turn also affects the char structure and thus the char reactivity; and 2) the heating rate of the fuel particles, which also affects the char structure.

Given the variability of char reactivities observed for different types of biomass under varying conditions, it is not appropriate to apply kinetic and structural parameters from the literature to conditions and biomasses for which they were not determined. Furthermore, Qin and Thunman [39] have shown that, given a specific type of biomass, a significant intrinsic heterogeneity in terms of reactivity exists from particle to particle, which means that to achieve statistically robust results, one must use either a batch test with a sufficient number of particles or a sufficiently high number of single particle tests.

Despite the numerous studies that have been conducted on the effects of the heating rate on char reactivity, the influence of the heat transfer conditions in a fluidized bed during pyrolysis remains to be established. Moreover, although the char location in the bed strongly influences the mass and heat transfer rates to the char and thus the char structure, its effect on the char reactivity and the resulting char gasification rate remains largely unknown. This knowledge is important not only in terms of understanding the conversion process, but also for the design of experiments where the aim is to quantify the kinetic and structural data needed for modelling of the gasification process.

The aim of the present work was to investigate the effects of the surrounding conditions on the char gasification rate in a FB unit. The conditions investigated were the fuel axial location during pyrolysis and char gasification, the pyrolysis atmosphere (i.e., the composition of the fluidizing gas during pyrolysis: N_2 or a N_2/ H_2O mixture), cooling of the char after pyrolysis, the fuel size, and the fuel concentration. Wood pellets and wood chips were used as fuels, and conditions relevant to DFBG, i.e., no O_2, were applied.

2 Experiments

2.1 Experimental Set-up and Procedures

The experiments were carried out in a 7-cm (inner diameter) bubbling fluidized bed reactor. A schematic of the experimental setup is shown in Fig. 2, and data relevant to the experimental set-up are listed in Table 1. In this set-up, distilled water (1) is transported at a controlled rate by a water pump (2) to a steam generator (3). The flow rate of N_2 (or air during combustion) is set using a mass flow regulator (4), and the gases are preheated in the preheating zone (5) before entering the reactor through a perforated ceramic plate (6), above which the fluidized bed (7) is located. To measure the fuel particle temperature, a K-type thermocouple is inserted into the center of one of the pellets (8) through a drilled hole.

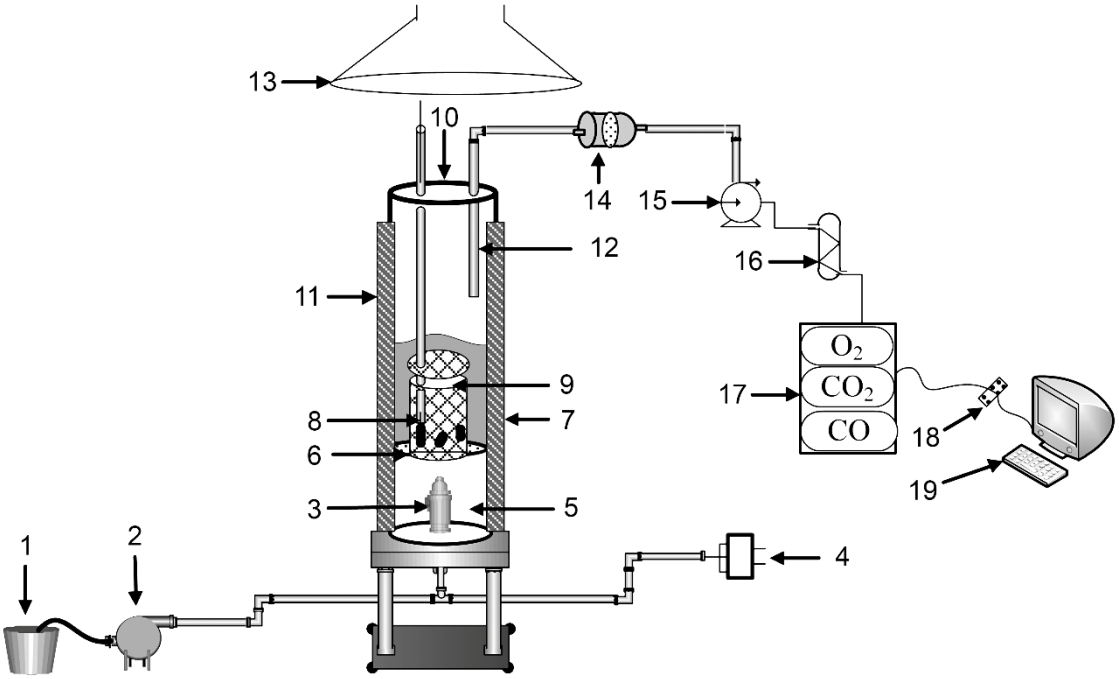

1-water tank, 2-water pump, 3-inbuilt steam generator, 4-mass flow regulator, 5-gas preheater, 6-perforated ceramic plate, 7-sand bed, 8-thermocouple inserted into pellet, 9-wire-mesh basket, 10-fuel inlet when basket is not used, 11-heating elements, 12-gas probe, 13-exhaust hood, 14-particle filter, 15-gas pump, 16-condenser, 17-gas analysers, 18-PC logger, 19-computer

Figure 2. Experimental set-up.

A wire-mesh basket with a lid (9) is used to control the position of the fuel during pyrolysis and char gasification. The position of the basket can be adjusted during the course of an experiment. In experiments in which the basket arrangement is not used, the fuel particles are inserted directly into the dense bed from the top of the reactor (10).

Table 1 . Experimental data.

Experimental parameter	
Inner diameter of reactor	7 cm
Total reactor height	140 cm
Height of preheating zone	60 cm
Mass range of inert bed material	400–600 g
Composition of bed material	91% SiO_2, 5% Al_2O_3 and 2% K_2O[a]
Bed material mean sauter diameter	350 μm
Bed material density	2500 kg/m^3
Bed height, range	4–6 cm
Size of openings in wire-mesh basket	0.8 mm
LA analyser CO_2, range and accuracy	0–20%$_{vol}$ ± 0.47 pp
LA analyser CO, range and accuracy	0–30,000 ppm ± 714.92 ppm
HA analyser CO_2, range and accuracy	0–5%$_{vol}$ ± 0.27 pp
HA analyser CO, range and accuracy	0–20,000 ppm ± 296.06 ppm

[a]present as feldspar

The reactor is electrically heated by heating elements (11) located on the reactor walls. A K-type thermocouple inserted into the dense bed of the reactor is used to measure the bed

temperature, which is controlled by a temperature regulator connected to the heating elements on the reactor walls. A gas probe (12) is used to sample a slip stream, while the remainder of the generated gas enters the exhaust hood (13). The sampled gas is transferred through a particle filter (14) via a gas pump (15). The gas then passes through a condenser, where the steam and tars are condensed (16), before reaching the gas analysers (17), which measure the concentrations of CO, CO_2, and O_2. Two types of gas analysers are used to measure the concentrations of CO and CO_2, one that is high-range with a lower level of accuracy (LA) and one that is low-range with higher level of accuracy (HA) (see Table 2 for details about the analysers). The output from the gas analysers is transformed using a PC logger (18) and the data are logged on a computer (19) every fifth second.

Table 2. Gas analysers used in the experiments.

Gas analysed	Name of Instrument	Measurement method	Range	Accuracy
CO_2	Rosemount, BINOS 100	NDIR	0–20 %	± 0.47 % [a]
CO_2	X-Stream	NDIR	0–5 %	± 0.27 % [b]
CO	Rosemount, BINOS 100	NDIR	0–30000 ppm	± 714.92 ppm[a]
CO	X-Stream	NDIR	0–20000 ppm	± 296.06 ppm[b]
O_2	Ankersmid Portable System APS	Paramagnetism	0–25 %	± 0.32 %

[a]Hereby denoted “Low Accuracy” (LA)
[b]Hereby denoted “High Accuracy” (HA)
NDIR: Non-dispersive infra-red

The experimental matrix is presented in Table 3. Pure N_2 was initially used as the fluidizing gas to allow pyrolysis of the fuel, which was inserted into the pre-heated reactor (except for Exp. 14, in which a mixture of 89%$_{vol}$ H_2O and 11%$_{vol}$ N_2 was used during pyrolysis). After approximately 3 minutes, which ensured complete pyrolysis (pyrolysis was assumed to be complete when the CO and CO_2 concentrations fell below the accuracy of the gas analysers), the gas flow into the reactor was switched to a mixture of H_2O and N_2 (see Table 3), to allow char gasification. After a given retention time (25 minutes for Exps. 1–12, and 11–22 minutes for Exps. 13–16), the experiment was terminated and air was used to combust any remaining char, while still monitoring the CO and CO_2 concentrations to allow closure of the carbon balance. When the basket was used, it was removed from the reactor prior to char combustion, and the char that remained in the basket was weighed.

Two different types of experiments were conducted: experiments using the basket (Exps. 2–9 and 11–12); and experiments without the basket (Exps. 1, 10, and 13–16). When the basket was not used, the particles could move freely within the fluidized bed (*F* is used to designate ‘Free’ in Table 3). When the basket was used, the axial location of the particles could be controlled; the basket could be arranged so that it was completely immersed in the dense bed (*IB* for ‘In Bed’ in Table 3) or so that it was only partly covered, allowing the fuel particles to rest on the surface of the bed (*BS* for ‘Bed Surface’ in Table 3). It was also possible to change

the position of the basket during the course of an experiment, so that pyrolysis and char gasification could take place at different positions. The basket could be removed from the reactor after pyrolysis to allow cooling of the char particles (Exps. 6–9). Pure N_2 was used to cool the char to room temperature, and the char was then weighed to estimate the char yield. The remaining char fines in the reactor were combusted before char gasification was started.

Two different softwood fuels were used (Fig. 3): wood pellets (WP); and wood chips (WC) (see Table 4 for fuel analysis and Table 5 for the principal metallic compounds in the fuels). The wood chips were dried prior to the experiments, which explains the low moisture content. The diameter of the wood pellets was 8 mm, with lengths in the range of 13–20 mm. Preliminary tests showed that good repeatability (the variation of the conversion degree with time was within ± 5%) was achieved using ten pellets, which is in agreement with Qin and Thunman [39], who reported that ten biomass samples gave a good representation of the average reactivity of a batch of pellets. Therefore, with the exception of Exp. 15, ten pellets were used in each experiment. In order to investigate how the char gasification rate is affected by the fuel concentration (i.e., the number of pellets), five pellets were used in Exp. 15. In Exp. 16, the wood pellets were "crushed" prior to pyrolysis, so that the largest dimension of each particle was < 7 mm. The wood chips varied widely in size (Fig. 3b).

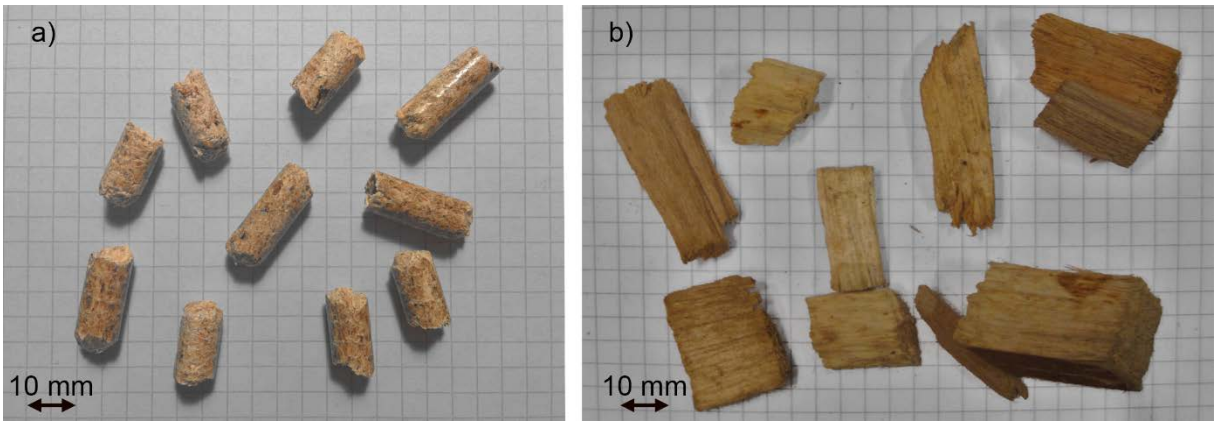

Figure 3. Fuel prior to experiments: a) wood pellets; and b) wood chips.

The fluidization velocity during pyrolysis was 0.26 m/s ($6 \cdot u_{mf}$), whereas it was somewhat higher during char gasification (0.37 m/s, $8 \cdot u_{mf}$). Experiments 1–12 were run with a steam concentration of $72\%_{vol}$ and a desired temperature of 840ºC, whereas in Exps. 13–16 the corresponding values were $89\%_{vol}$ and 850ºC, respectively. The time-averaged temperatures attained during pyrolysis and char gasification in each run are listed in Table 3. For the experiments aimed at a temperature of 840ºC, 96% of the measured points during char gasification were within ±5ºC, whereas 91% were within ±10ºC during pyrolysis. For the experiments conducted at 850ºC, 96% of the measurement points were within ±10ºC during char gasification and 89% were within ±15ºC during pyrolysis.

Table 3. Experimental matrix.

Exp.	Fuel mass (g)	Fuel type	No. of Pellets	T_{av} P/CG (ºC)	X_{H2O} ($\%_{vol}$)	BC P	BC CG	Cooling after P	P gas	Carbon balance (%)
1	8.51	WP	10	846/841	72	F	F	No	N_2	104
2	8.50	WP	10	827/840	72	IB	IB	No	N_2	115
3	8.52	WP	10	842/842	72	IB	BS	No	N_2	109
4	8.49	WP	10	840/841	72	BS	IB	No	N_2	108
5	8.52	WP	10	842/841	72	BS	BS	No	N_2	109
6	8.50	WP	10	841/842	72	IB	IB	Yes	N_2	110
7	8.48	WP	10	840/841	72	IB	BS	Yes	N_2	115
8	8.51	WP	10	841/841	72	BS	IB	Yes	N_2	114
9	8.48	WP	10	843/841	72	BS	BS	Yes	N_2	105
10	8.52	WC	-	847/840	72	F	F	No	N_2	97
11	8.52	WC	-	842/841	72	IB	IB	No	N_2	127
12	8.53	WC	-	842/840	72	BS	IB	No	N_2	113
13	9.97	WP	10	850/856	89	F	F	No	N_2	-
14	9.95	WP	10	840/851	89	F	F	No	H_2O-N_2	-
15	4.98	WP	5	845/853	89	F	F	No	N_2	96
16	10.01	WP	10 crushed	833/854	89	F	F	No	N_2	-

Abbreviations used: WP, wood pellets; WC, wood chips; P, pyrolysis; CG, char gasification; BC, boundary conditions; F, free; IB, inside the dense bed; BS, on the bed surface.

Table 4 . Fuel analysis for the wood pellets and wood chips.

	Wood pellets	Wood chips
HHV (MJ/kg)	20.12	19.65
LHV (MJ/kg)	18.77	18.36
Moisture ($\%_{wt}$)	8.83	0.6
Ash ($\%_{wt,db}$)	0.4	0.5
C ($\%_{wt,db}$)	49.7	49.7
H ($\%_{wt,db}$)	6.2	5.9
N ($\%_{wt,db}$)	0.07	0.16
S ($\%_{wt,db}$)	< 0.02	< 0.02
Cl ($\%_{wt,db}$)	< 0.01	< 0.01
O ($\%_{wt,db}$) (from difference)	44	44

Table 5 . Principal metallic compounds in the wood pellets and wood chips (dry basis).

	Wood pellets (mg/g)	Wood chips (mg/g)
Al	5	1
Si	21	4
Fe	5	1
Ti	< 1	< 1
Mn	12	6
Mg	17	23
Ca	120	150
Ba	2	2
Na	4	3
K	50	88
P	7	15

Some additional pyrolysis experiments, P1–P5, were conducted to estimate the char yields and the heating rates of the wood pellets. For these experiments, the pellets were dried prior to

pyrolysis. Ten pellets were used and the mass of each batch of dried pellets was 9 ± 0.2 g. Aside from this, these experiments were conducted in the same way as Exps. 6–9, albeit without char gasification. The basket was used and in P1–P3, the pellets were placed inside the dense bed (IB), while in P4 and P5 the pellets were located on the bed surface (BS).

BET surface analysis with N_2 was carried out on char samples extracted from the reactor after char gasification. The samples were dried at 105ºC for 90 minutes prior to analysis. The instrument used (Micromeritics ASAP 2020) can measure pore sizes of between 0.3 nm and 0.3 µm, so it covers the entire range of mesopores (2–50 nm [40]), whereas its capability is limited regarding micropores and macropores. A scanning electron microscope (SEM) was also used to investigate the pore structures of the char samples.

A limitation of the present work is that the pyrolysis and char conversion were separated in time. Thus, any influence on the char gasification rate of volatile species in the environment of the fuel particle (such as decreased gasification rate due to the inhibitory effects of H_2 and CO) is disregarded. However, given the relatively rapid rate of pyrolysis (as compared to lateral fuel mixing), it seems likely that most of the volatiles are released in the area close to the fuel feeding ports of a FB, whereas char gasification occurs throughout the cross-section of the bed, owing to its relatively low conversion rate. Furthermore, the dispersive lateral fuel mixing induced by the bubble flow in a FB [3, 41] can to some extent be controlled by the superficial velocity [42] or by introducing baffles into the reactor [5]. Thus, there are zones within a FB where the char gasification rate is maximised due to the absence of volatile species. With the maximal char gasification rate setting the upper limit for char conversion, the present work studies this extreme case, in which pyrolysis and char gasification are not co-existing but separated in time.

Another limitation is that since Exps. 1–12 all have the same retention time (25 minutes), the degrees of char conversion are not identical at the end of the experiments. The total surface area and pore structure change during the conversion process, which means that it is not possible to exclude an effect of the degree of char conversion on the results of the analyses of the BET surface area, SEM, and char fragmentation.

2.2 Data Processing

The HA analyser was used to measure CO concentrations up to $2\%_{vol}$ and CO_2 concentrations up to $5\%_{vol}$. When the concentrations of these gases were outside the limits of the HA analyser, the LA analyser was used. As shown in Fig. 4, there is a consistent difference between the values measured by the two analysers at $Y_{CO2} < 5\%_{vol}$.

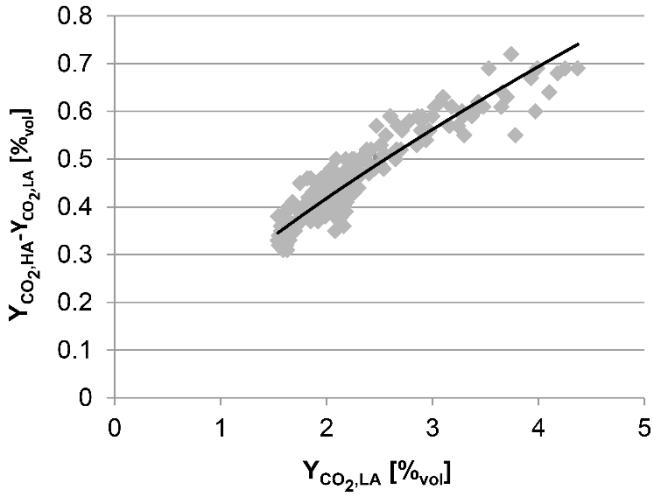

Figure 4. Comparison of the CO_2 concentrations given by the LA analyser (grey squares) and the function described in Eq. (2) (black curve, $R^2 = 0.864$).

Equation (2) gives a rather good fit to the data-points in Fig. 4 (black curve):

$$Y_{CO_2,HA} - Y_{CO_2,LA} = 0.2515 \cdot {Y_{CO_2,LA}}^{0.732} \tag{2}$$

This equation was used to correct the CO_2 measurements obtained with the LA analyser. Use of the LA analyser was necessary for 15% of the measurement points for char gasification in Exps. 13–16. During combustion, the limit of the HA analyser was exceeded for 11% of all the measurement points. For CO, the difference between the measurements given by the two instruments was negligible, and the value of $Y_{CO,LA}$ could be used directly when the CO concentration exceeded 2%$_{vol}$. The highest concentrations of CO_2 and CO measured by the LA analyser were 12.0%$_{vol}$ and 2.9%$_{vol}$, respectively.

The two relevant reactions taking place in the reactor are char gasification (R1) and the water-gas-shift reaction (R2):

$$C + H_2O \rightarrow CO + H_2 \tag{R1}$$

$$CO + H_2O \leftrightarrow CO_2 + H_2 \tag{R2}$$

Thus, the dry gas during char gasification is assumed to consist of CO, CO_2, H_2, and N_2. The mass flow of carbon leaving the reactor is calculated according to:

$$\dot{m}_{C,out}(t) = \frac{\dot{n}_{N_2}}{Y_{N_2}(t)}\left(Y_{CO}(t) + Y_{CO_2}(t)\right)M_C \tag{3}$$

By setting up the elemental mass balances for O and H, the fraction of H_2 on a dry basis can be calculated, which in turn makes it possible to calculate the fraction of N_2, Y_{N2}, from the mass fraction constraint. It is assumed that the ash-free char consists of pure carbon.

The char yield can be estimated for Exps. 6–9, where the basket is removed from the reactor after pyrolysis to allow cooling before char gasification:

$$Y_{ch} = \frac{m_{ch,P} + m_{ch,f}}{m_0} \quad (4)$$

Here, $m_{ch,P}$ is the mass of ash-free char remaining in the basket after pyrolysis. The term $m_{ch,f}$ refers to the mass of ash-free char left in the reactor, as a result of fine particles escaping through the holes in the wire-mesh basket (fines); it was determined by combusting the fines and measuring the CO_2 and CO concentrations in the combustion gas. The accuracy of determining the mass of ash-free char after pyrolysis was relatively high (± 0.07%), since the char particles were all intact after pyrolysis. However, there is some uncertainty regarding the mass of fines left in the reactor after pyrolysis, related to the accuracy of the analysers (Table 2). It should be noted that the char yields had to be assumed when calculating the reactivities of non-cooled wood pellets, i.e., in Exps. 1–5 and 13–16, as the basket was not removed between the pyrolysis and char gasification steps in these cases. The char yield of the wood chips also had to be assumed for the calculations of the gasification rate in Section 3, since no experiments that entailed cooling after pyrolysis were carried out for the wood chips. Char from wood chips, produced with low heating rates in a TGA (< 0.15 ºC/s, calculated according to Eq. (5), gave char yields of between 17.0%$_{wt}$ and 18.4%$_{wt}$, which should be higher than the yields of chars produced in a fluidized bed owing to the higher heating rate of the fluidized bed. Therefore, the TGA value of 17%$_{wt}$ was taken as a conservative approach for the upper limit for the char yield of wood chips.

The instantaneous heating rate of the fuel particles, *HR*, is calculated according to:

$$HR(t) = \frac{T_F(t) - T_{F,0}}{t} \quad (5)$$

The degree of char conversion, *X*, is defined as:

$$X(t) = \frac{m_0 Y_{ch} - m_C(t)}{m_0 Y_{ch}} \quad (6)$$

The definition of the char gasification rate used in this work is the conversion rate, R_m, which is normalised with the initial mass of the char particle:

$$R_m = \frac{dX(t)}{dt} = -\frac{1}{m_0 Y_{ch}} \frac{dm_C(t)}{dt} = \frac{\dot{m}_{C,out}(t)}{m_0 Y_{ch}} \quad (7)$$

The carbon balance is obtained by first calculating the total amount of carbon leaving the reactor during char gasification ($m_{C,G}$) and combustion of the remaining char ($m_{C,C}$), from the measured concentrations of CO and CO_2. Elutriation of char fines is assumed to be negligible. For experiments in which a basket is used, the residual mass of ash-free char inside the basket after char gasification ($m_{ch,CG}$) is also considered. This mass is then divided by the initial mass of ash-free char, $m_0 Y_{ch}$:

$$C_b = \frac{m_{C,G} + m_{C,C} + m_{ch,CG}}{m_0 Y_{ch}} \quad (8)$$

The accuracy of the carbon balance is shown in Table 3. For Exps. 1, 10 and 15, the balance closure is almost achieved. In the experiments in which a basket was used (Exps. 2–9 and 11–12), the measured carbon exceeded the amount of fed carbon (closure values in the range of 105%–127%), due to an overestimation of $m_{ch,CG}$ caused by bed material adhering to the char (roughly estimated, on average 50% of $m_{ch,CG}$ originates from the bed material). When the particle filter was inspected after the experiments it was found to contain a low level of char (it mainly contained condensed tars), supporting the decision to neglect elutriation of char fines in the carbon balance.

3 Results and Discussion

Figure 5 shows the heating rates (Eq. (5)) of the pellets in Exps. P3, P4, 2, and 4 as a function of the instantaneous fuel temperature, $T_F(t)$, based on the temperature measured at the centre of a fuel particle by a thermocouple inserted into the studied pellet.

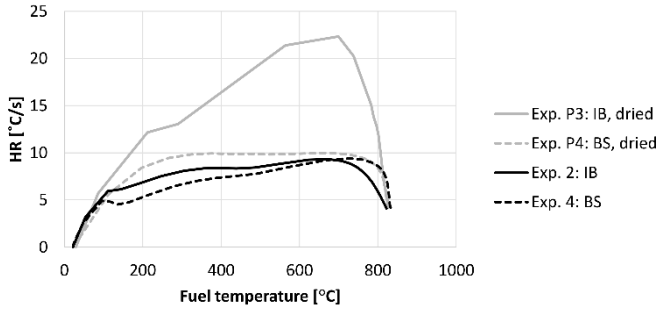

Figure 5. Heating rate of wood pellets as a function of the instantaneous fuel temperature for Exps. P3, P4, 2, and 4.

It is clear that the heating rates are higher for the two cases in which the pellets were dried prior to pyrolysis (Exps. P3 and P4). The heating rate for Exp. P3 (pyrolysis in the dense bed) is up to 2.2-fold higher than that for P4 (pyrolysis on the bed surface) due to the higher heat transfer provided by the inert bed material. The same trend can be observed for the pellets that were not dried prior to pyrolysis: the heating rate is higher for Exp. 2 (pyrolysis in the dense bed) during most of the heating process (20ºC–700ºC), although the difference is relatively small (at most, the heating rate for Exp. 2 is around 1.5-fold higher than that for Exp. 4). The heating rates shown in Fig. 5 are much lower than those typically observed for the pyrolysis of millimetre-sized fuel particles in a fluidized bed (100ºC/s–500ºC/s) [15]. This is explained by the fact that the temperature was measured at the centre of the particle, combined with the relatively high internal resistances to heat transfer and thermal inertia of the large particles used in the present tests. Thus, there will be a great variation in heating rates within a particle, and it is possible that the difference in heating rates is more pronounced at the surface of the particles.

Table 6 shows the BET surface areas, as well as the percentages of micropore area for the wood pellets and wood chips subjected to different boundary conditions. There were no significant differences between the non-cooled cases (Exps. 2, 4, and 5) and the cooled samples (Exps. 7–9). It is evident that the BET surface area for the wood chips (Exps. 11 and 12) is significantly lower than that for the wood pellets. This is likely due to the fact that wood chips have a higher number of large macropores than wood pellets, which cannot be measured by gas adsorption (see Fig. 7). In addition, having a relatively low number of large pores rather than many small pores leads to a smaller total surface area.

Table 6 . Degrees of char conversion, BET surfaces area and the percentages of micropore area after 25 minutes of char gasification of wood pellets and wood chips subjected to different boundary conditions.

Exp.	Boundary conditions	Fuel category	Degree of char conversion (%)	BET surface area (m^2/g)	Percentage of micropore area (%)
2	IB/IB	WP	87	1334	17
4	BS/IB	WP	63	1169	22
5	BS/BS	WP	87	1581	11
7	IB/BS	WP, cooled	88	1493	15
8	BS/IB	WP, cooled	62	1231	19
9	BS/BS	WP, cooled	81	1224	11
11	IB/IB	WC	82	469	14
12	BS/IB	WC	73	489	23

For wood pellets, the BET surface area was fairly similar for all the investigated cases, although it was slightly higher for Exps. 5 and 7. However, the percentage of micropore area differed significantly between the samples. Both Exp. 5 (pyrolysis and char gasification on the bed surface) and its equivalent cooled case, Exp. 9, showed rather low percentages of micropores (11%), whereas Exps. 4, 8 and 12 (pyrolysis on the bed surface and char gasification inside the dense bed) had the highest percentages of micropores (22%, 19%, and 23%, respectively).

Table 7 shows the char yields, including the range of uncertainty and the levels of fines on a dry ash-free basis calculated for Exps. 6–9, where the char pellets were removed from the reactor after pyrolysis.

Table 7 . Char yields and levels of fines for cooled wood pellets.

Exp.	Dried prior to pyrolysis	BC during pyrolysis	Y_{ch} ($\%_{wt}$)	$m_{C,f}/m_0$ ($\%_{wt}$)
6	No	IB	19.0 ± 0.1	1.2
7	No	IB	22.0 ± 0.7	2.6
8	No	BS	18.6 ± 0.07	0.59
9	No	BS	18.3 ± 0.07	0.41
P1	Yes	IB	16.3 ± 0.2	1.53
P2	Yes	IB	16.2 ± 0.2	1.57
P4	Yes	BS	16.3 ± 0.1	0.66
P5	Yes	BS	16.9 ± 0.09	0.61

As shown in Table 7, the surrounding conditions during pyrolysis do not seem to have had a significant impact on the char yields. The char yields of the dried pellets (Exps. P1–P5) were all very similar, and somewhat lower than those of the wet pellets (Exps. 6–9). The conversion of the dry pellets was characterised by higher heating rates (Fig. 5), which could be a reason for the difference in char yield. For the wet pellets, the char yield was 18–19%$_{wt}$ for three of the experiments, whereas for Exp. 7 it was somewhat higher. It should be noted also that the amount of fines was significantly higher in Exp. 7 (about 6-fold higher than in Exp. 9), resulting in a higher level of uncertainty. Since wet pellets were used in Exps. 1–5, the average of the char yields obtained in Exps. 6, 8, and 9 was used (18.6%$_{wt}$) to estimate the char yield needed for the calculations linked to these experiments. With the exception of Exp. 7, the repeatability of the char yields reported in Table 7 was good; for this reason, the char yield in Exp. 7 was omitted from the calculation of the average char yield.

Figure 6 shows the char gasification rate, R_m, for Exps. 1–12, calculated by time-averaging five measurement points (equivalent to 25 s) around X = 20%. The error bars for Exps. 1–9 include the uncertainty related to the accuracy of the HA analyser. For Exps. 1–5, the error bars additionally include the uncertainties of the char yields presented in Table 7 for Exps. 6, 8, and 9 (Y_{ch} = 18.2–19.1%$_{wt}$). The char yield for the wood chips had to be assumed when calculating the gasification rate, as discussed in Section 2.2. The error bars for Exps. 10–12 in Fig. 6 show the range of gasification rates obtained for char yields between 14%$_{wt}$ and 17%$_{wt}$. These bars also take into account the uncertainty in the accuracy of the HA analyser. A value of 15%$_{wt}$ gives the best closure of the carbon balance for Exp. 10 (in which the char remaining in the reactor after gasification was combusted), so this value was chosen when calculating the data-points for Exps. 10–12.

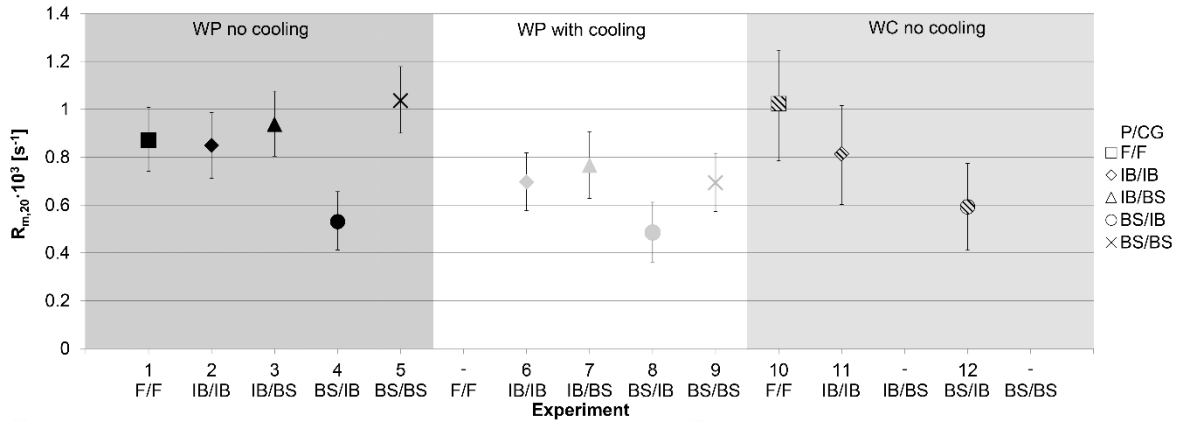

Figure 6. Char gasification rates at X = 20% in Exps. 1–12. Symbols used: black, wood pellets (WP) without cooling; grey, WP with cooling; striped, wood chips (WC) without cooling; P, pyrolysis; CG, char gasification; F, free; IB, inside the dense bed; BS, on the bed surface.

The results shown in Fig. 6 are divided into three fuel categories: char from non-cooled wood pellets; char from wood pellets that were subjected to cooling prior to char gasification; and char from non-cooled wood chips. As expected, cooling decreased the gasification rate of the char, although the effect observed in the present work (8%–33% decrease) is small compared to that reported in other studies (decreases in the range of 48%–83%) [13, 43]. The gasification rates of char from wood pellets and wood chips converted under the same

conditions are rather similar, which is in line with the fact that the ash content and composition were comparable for the two fuels (see Tables 4 and 5, respectively), although the wood chips had somewhat higher concentrations of K and Ca. The relatively large level of uncertainty of the rates for the wood chips should be noted.

Comparing the char gasification rates for non-cooled wood pellets using the basket arrangement (Exps. 2–5), it is clear that the gasification rate in Exp. 4, during which pyrolysis occurred on the bed surface and char gasification inside the dense bed, is significantly (1.6–2.0-fold) lower than the corresponding rates in Exps. 2, 3, and 5, which are all relatively similar. The same trends, albeit weaker, are evident for the cooled wood pellets (R_m for Exp. 8 is 1.4–1.6-fold lower than R_m for Exps. 6, 7, and 9) and the wood chips, for which R_m of Exp. 12 is 1.4-fold lower than that of Exp. 11.

The results shown in Fig. 6 can be explained by evaluating if the char pore structure resulting from each experiment underwent mechanisms enhancing its reactivity, as well as decreasing its resistance to internal diffusion. Exemplifying the results with those for wood pellets without cooling (Exps. 2–5), fuels that underwent pyrolysis inside the dense bed (Exps. 2 and 3) were subjected to a comparatively high heating rate (Fig. 5), resulting in relatively porous char with a larger amount of meso- and macropores, thus more reactive than those produced on the bed surface and with a lower resistance to internal diffusion. For the chars pyrolysed on the bed surface, char undergoing gasification on the bed surface (Exp. 5) experienced a relatively high steam-char contact compared to that immersed in the bed during char gasification (Exp. 4), yielding a higher increase in porosity and thus higher char reactivity and a lower resistance to internal diffusion. This is supported by the char structural analysis (Table 6); the content of micropores was 1.5–2.0-fold higher in chars that were subjected to a low heating rate during pyrolysis followed by a low steam-char contact during char gasification (Exp. 4) than otherwise.

For wood pellets, when no basket was used (Exp. 1), the gasification rate was 1.6-fold higher than that in Exp. 4 (Fig. 6). Therefore, it seems unlikely that the free char particles underwent pyrolysis on the bed surface and char gasification inside the dense bed. Since the gasification rate in Exp. 1 is rather similar to the corresponding rates in Exps. 2, 3, and 5, it is not possible to determine the positions of the free pellets during pyrolysis and char gasification. However, considering the behaviour of the wood pellets, as observed by Berdugo Vilches et al. [37], the degree of vertical mixing should be rather high at the high superficial velocities (6-8·u_{mf}) used in the present work, making it likely that the free pellets (Exp. 1) populated most of the vertical extension of the bed (the conditions applied in Exp. 2) rather than gathering on the bed surface during pyrolysis and char gasification. However, for wood chips, the gasification rate of the free fuel particles (Exp. 10) is apparently higher than that for the IB/IB case (Exp. 11). This indicates that the char gasification in Exp. 10 took place on the bed surface (which is likely, since the density of the wood chips is lower than that of the wood pellets), where the level of steam-char contact is higher, resulting in a higher gasification rate.

Figures 7 and 8 show SEM images of the chars after 25 minutes of char gasification. Figure 7 compares the wood pellets and wood chips (Exps. 2 and 11, respectively) that have undergone

both pyrolysis and char gasification inside the dense bed. As expected, the wood chips have large, regular pores, whereas the wood pellets seem to have undergone plastic deformation.

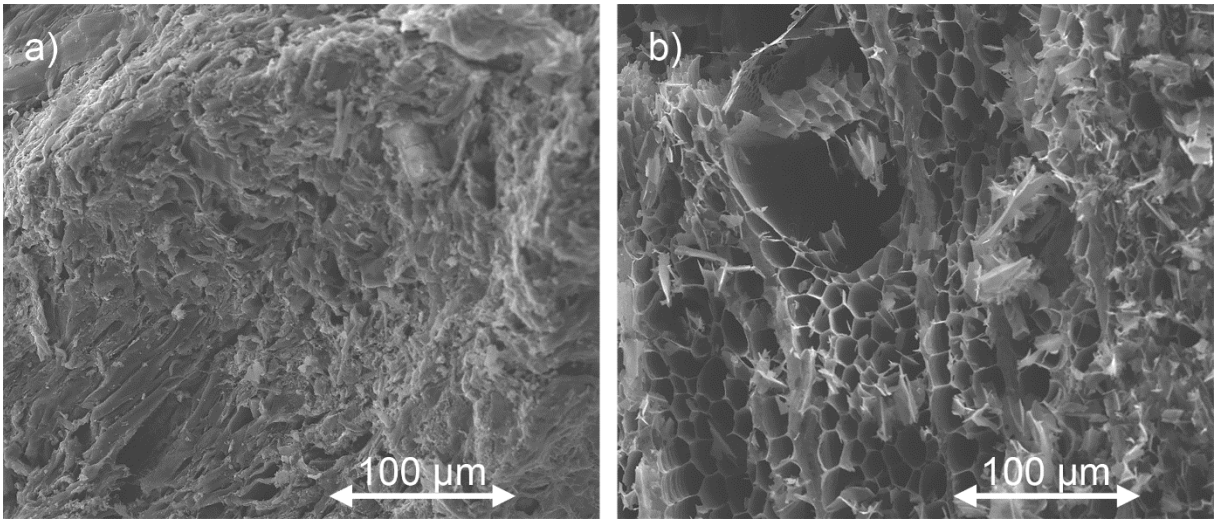

Figure 7. SEM images (400×magnification) for the IB/IB case for: a) wood pellets, Exp. 2; and b) wood chips, Exp. 11.

As seen in Figs. 7and 8, the char from the wood pellets subjected to different surrounding conditions exhibit slightly different pore structures; for instance, the char from Exp. 4 (Fig. 8a) is more compact than the chars obtained from Exps. 5 (Fig. 8b) and 7 (Fig. 8c).

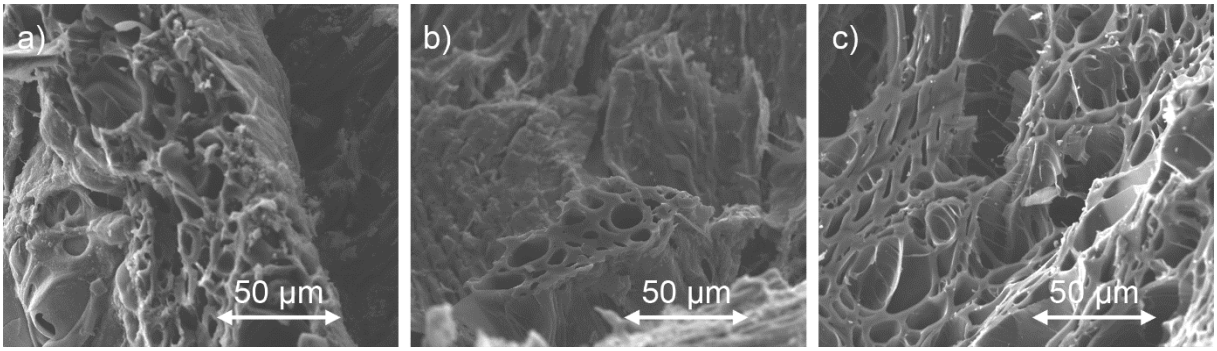

Figure 8. SEM images (800×magnification) for WP char for: a) Exp. 4 (BS/IB); b) Exp. 5 (BS/BS); and c) Exp. 7 (IB/BS, cooled).

Figure 9 shows the char that remained inside the basket after 25 minutes of char gasification in Exps. 8 and 9 (pyrolysis on the bed surface in both experiments). Char that was gasified on the bed surface (Exp. 9, Fig. 9b) underwent a greater degree of char conversion (X = 81%) and a higher level of char fragmentation than char that was gasified inside the dense bed, for which the degree of char conversion after 25 minutes was X = 62% (Fig. 9a). It should be noted that all ten pellets were intact after pyrolysis for Exps. 6–9.

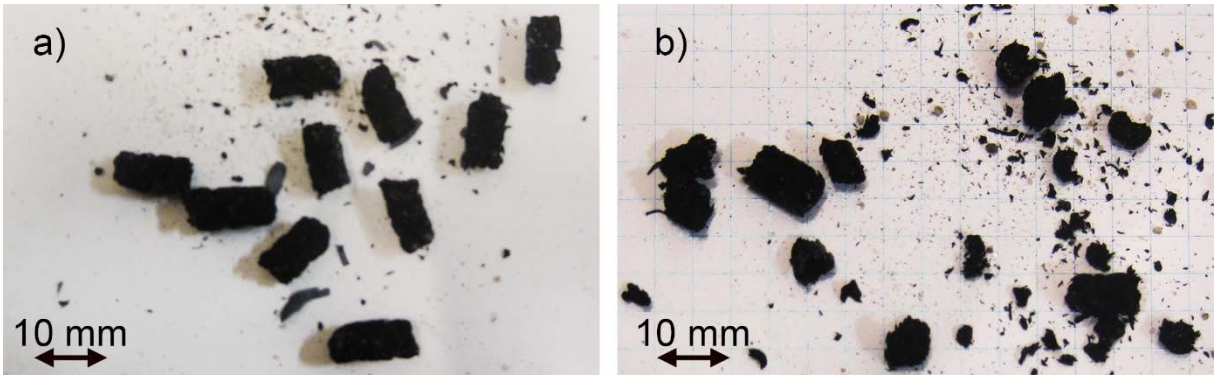

Figure 9. Appearance of cooled WP char after 25 minutes of char gasification in a) Exp. 8 (BS/IB) and b) Exp. 9 (BS/BS).

Figure 10 shows the gasification rate, R_m, as a function of the degree of char conversion for Exps. 13–16. Experiment 13 can be regarded as the base case, involving ten whole pellets with a pyrolysis atmosphere of pure N_2.

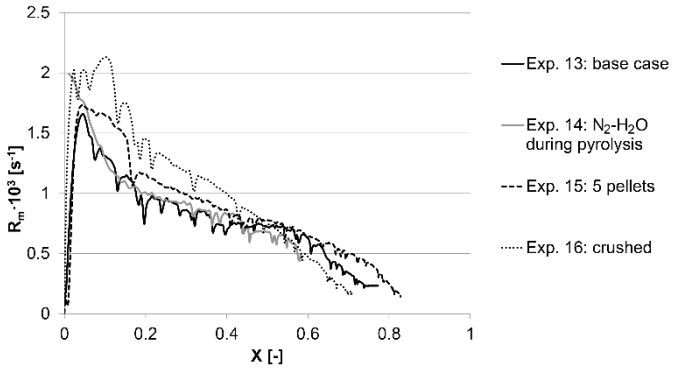

Figure 10. Gasification rates as a function of the degree of conversion of wood pellets for Exps. 13–16.

As seen in Fig. 10, crushing the pellets (Exp. 16) yielded a higher gasification rate for X < 50% compared to the base case (Exp. 13), although its decrease with the degree of char conversion is also much higher for X = 10–60%. Lundberg et al. [44] reported that diffusion effects disappeared at X > 20% for the conditions used in Exps. 13, 15, and 16, implying that the effect of the fuel size on the char gasification rate observed in Fig. 10 for X > 20% should be attributed to structural effects rather than to diffusion effects (see Fig. 1). This indicates that the reduction in particle size often used when determining the reactivity parameters and structural models of char conversion is problematic.

Comparing the cases with five pellets (Exp. 15) and ten pellets (Exp. 13) in Fig. 10, it can be seen that the gasification rate is slightly higher for the case with five pellets during most of the conversion process. This may reflect the effect of fuel composition variability, as described above, which is more prominent in smaller batches of fuel. In parallel, another possible explanation for the higher gasification rate observed when five pellets were used is that the inhibitory effect of H_2 is lower when fewer particles are used: five pellets generate less H_2 during char gasification than ten pellets, thus leading to a lower H_2 concentration and thereby,

a lower level of H_2 inhibition [11]. This indicates that H_2 inhibition may be an issue when low fluidization velocities are used in a DFBG unit, since this leads to high fuel concentrations as the fuel gathers on the bed surface, as discussed above.

In Exp. 14, the pyrolysis atmosphere consisted of a mixture of N_2 and H_2O, whereas it consisted of pure N_2 in Exp. 13. A comparison of these two experiments (Fig. 10) reveals that the pyrolysis atmosphere does not significantly affect the char gasification rate. This indicates that a pyrolysis atmosphere consisting of N_2 can be used without compromising the accuracy of the results.

4 Conclusions

The influence of the surrounding conditions and fuel size on the rate of char gasification in a fluidized bed were investigated. Tests were carried out under conditions relevant to DFBG, in which inhibition by volatiles was disregarded in order to focus on the maximal attainable char gasification rate. The fuel axial location could be controlled so that the fuel particles were either inside the dense bed or on the bed surface.

When pyrolysis on the bed surface was followed by char gasification inside the dense bed, the char gasification rate was up to 2-fold lower than the other three studied combinations of the fuel axial location, all of which had similar char gasification rates. This is attributed to the difference in heating rate and steam-char contact experienced by the fuel inside the dense bed and at the bed surface, which in turn affect the structure of the char formed. Due to the formation of endogenous bubbles, it is possible that pyrolysis occurs on the bed surface and that the char subsequently sinks into the dense bed again when pyrolysis is complete, fulfilling these conditions. Furthermore, cooling the char after pyrolysis resulted in lower char gasification rates for all the tested combinations of fuel locations during pyrolysis and char gasification.

Fuel particle size was found to affect both the gasification rate (the smaller the particle size, the higher was the gasification rate) and the dependence of the gasification rate on the degree of char conversion. This cannot be attributed entirely to diffusional effects. A parallel explanation is that the smaller particles have been subjected to higher heating rates and higher levels of steam-char contact, yielding more porous and thereby more reactive char particles.

Thus, it can be concluded that the operational conditions of a DFBG system, through modified fuel axial mixing, can influence the char reactivity and the resulting char gasification rate. Furthermore, experimental determination of reactivity data at the laboratory scale must account for the axial location of the fuel at the desired end-scale during the different parts of the conversion process, using similar fuel sizes.

Acknowledgements

This work has been financially supported by Svenskt Förgasningscentrum (SFC) and Energiforsk.

References

[1] Hofbauer H. Scale Up of Fluidized Bed Gasifiers from Laboratory Scale to Commercial Plants: Steam Gasification of Solid Biomass in a Dual Fluidized Bed System. FBC19. Vienna2006.

[2] Neubauer Y. 6 - Biomass gasification. In: Rosendahl L, editor. Biomass Combustion Science, Technology and Engineering: Woodhead Publishing; 2013. p. 106-29.

[3] Pallarès D, Johnsson F. Modeling of fuel mixing in fluidized bed combustors. Chemical Engineering Science. 2008;63:5663-71.

[4] Horio M. 1 - Overview of fluidization science and fluidized bed technologies. In: Scala F, editor. Fluidized Bed Technologies for Near-Zero Emission Combustion and Gasification: Woodhead Publishing; 2013. p. 3-41.

[5] Larsson A. Fuel conversion in a dual fluidized bed gasifier -experimental quantification and impact on performance: Chalmers University of Technology; 2014.

[6] Gunnarsson I. The GoBiGas Project; Technical Report. Göteborg, Sweden: Göteborg Energi; 2011.

[7] Tchoffor PA, Davidsson KO, Thunman H. Transformation and release of potassium, chlorine, and sulfur from wheat straw under conditions relevant to dual fluidized bed gasification. Energy Fuels. 2013;27:7510-20.

[8] Larsson A, Seemann M, Neves D, Thunman H. Evaluation of performance of industrial-scale dual fluidized bed gasifiers using the chalmers 2-4-MWth gasifier. Energy Fuels. 2013;27:6665-80.

[9] Lundberg L, Pallarès D, Johansson R, Thunman H. A 1-dimensional model of indirect biomass gasification in a dual fluidised bed system. 11th International Conference on Fluidized Bed Technology, CFB 2014. Beijing: Chemical Industry Press; 2014. p. 607-12.

[10] Mermoud F, Salvador S, Van de Steene L, Golfier F. Influence of the pyrolysis heating rate on the steam gasification rate of large wood char particles. Fuel. 2006;85:1473-82.

[11] Barrio M, Gøbel, B., Risnes, H., Henriksen, U., Hustad, J.E., Sørensen, L.H. Steam gasification of wood char and the effect of hydrogen inhibition on the chemical kinetics. In: Bridgwater AV, editor. Progress in Thermochemical Biomass Conversion. U.K.: Blackwell Science; 2001.

[12] Li F-h, Li Z-z, Huang J-j, Fang Y-t. Characteristics of fine chars from fluidized bed gasification of Shenmu coal. Journal of Fuel Chemistry and Technology. 2014;42:1153-9.

[13] Nilsson S, Gómez-Barea A, Cano DF. Gasification reactivity of char from dried sewage sludge in a fluidized bed. Fuel. 2012;92:346-53.

[14] Di Blasi C. Combustion and gasification rates of lignocellulosic chars. Progress in Energy and Combustion Science. 2009;35:121-40.

[15] Gómez-Barea A, Leckner B. Modeling of biomass gasification in fluidized bed. Progress in Energy and Combustion Science. 2010;36:444-509.

[16] Adschiri T, Shiraha T, Kojima T, Furusawa T. Prediction of CO2 gasification rate of char in fluidized bed gasifier. Fuel. 1986;65:1688-93.

[17] Bjerle I, Eklund H, Svensson O. Gasification of Swedish black shale in the fluidized bed. Reactivity in steam and carbon dioxide atmosphere. Industrial & Engineering Chemistry Process Design and Development. 1980;19:345-51.

[18] Scott SA, Davidson JF, Dennis JS, Fennell PS, Hayhurst AN. The rate of gasification by CO2 of chars from waste. Proceedings of the Combustion Institute. 2005;30:2151-9.

[19] Goring GE, Cursan, G.P., Tarbox, R. P., Gorin, E. Kinetics of Carbon Gasification by Steam. Industrial and Engineering Chemistry. 1952;44:1051-65.

[20] Liu H, Zhu H, Kaneko M, Kato S, Kojima T. High-temperature gasification reactivity with steam of coal chars derived under various pyrolysis conditions in a fluidized bed. Energy Fuels. 2010;24:68-75.

[21] Kojima T, Assavadakorn P, Furusawa T. Measurement and evaluation of gasification kinetics of sawdust char with steam in an experimental fluidized bed. Fuel Processing Technology. 1993;36:201-7.

[22] Nilsson S, Gómez-Barea A, Fuentes-Cano D, Campoy M. Gasification kinetics of char from olive tree pruning in fluidized bed. Fuel. 2014;125:192-9.

[23] Nilsson S, Gómez-Barea A, Ollero P. Gasification of char from dried sewage sludge in fluidized bed: Reaction rate in mixtures of CO2 and H2O. Fuel. 2013;105:764-8.

[24] Lahijani P, Zainal ZA, Mohamed AR, Mohammadi M. CO2 gasification reactivity of biomass char: Catalytic influence of alkali, alkaline earth and transition metal salts. Bioresource Technology. 2013;144:288-95.

[25] Perander M, DeMartini N, Brink A, Kramb J, Karlström O, Hemming J, et al. Catalytic effect of Ca and K on CO2 gasification of spruce wood char. Fuel. 2015;150:464-72.

[26] Mitsuoka K, Hayashi S, Amano H, Kayahara K, Sasaoaka E, Uddin MA. Gasification of woody biomass char with CO2: The catalytic effects of K and Ca species on char gasification reactivity. Fuel Processing Technology. 2011;92:26-31.

[27] Kannan MP, Richards GN. Gasification of biomass chars in carbon dioxide: dependence of gasification rate on the indigenous metal content. Fuel. 1990;69:747-53.

[28] Klinghoffer NB, Castaldi MJ, Nzihou A. Influence of char composition and inorganics on catalytic activity of char from biomass gasification. Fuel. 2015;157:37-47.

[29] Lahijani P, Zainal ZA, Mohamed AR, Mohammadi M. Ash of palm empty fruit bunch as a natural catalyst for promoting the CO2 gasification reactivity of biomass char. Bioresource Technology. 2013;132:351-5.

[30] Min F, Zhang M, Zhang Y, Cao Y, Pan W-P. An experimental investigation into the gasification reactivity and structure of agricultural waste chars. Journal of Analytical and Applied Pyrolysis. 2011;92:250-7.

[31] Cetin E, Moghtaderi B, Gupta R, Wall TF. Influence of pyrolysis conditions on the structure and gasification reactivity of biomass chars. Fuel. 2004;83:2139-50.

[32] Chen G, Yu Q, Sjöström K. Reactivity of char from pyrolysis of birch wood. Journal of Analytical and Applied Pyrolysis. 1997;40–41:491-9.

[33] Fushimi C, Araki K, Yamaguchi Y, Tsutsumi A. Effect of heating rate on steam gasification of biomass. 1. Reactivity of char. Ind Eng Chem Res. 2003;42:3922-8.

[34] Kumar M, Gupta RC. Influence of carbonization conditions on the gasification of acacia and eucalyptus wood chars by carbon dioxide. Fuel. 1994;73:1922-5.

[35] Rocca PAD, Cerrella EG, Bonelli PR, Cukierman AL. Pyrolysis of hardwoods residues: on kinetics and chars characterization. Biomass and Bioenergy. 1999;16:79-88.

[36] Sun K, Jiang Jc. Preparation and characterization of activated carbon from rubber-seed shell by physical activation with steam. Biomass and Bioenergy. 2010;34:539-44.

[37] Berdugo Vilches T, Sette, E., Thunman, H. Behaviour of biomass particles in a large scale (2-4MWth) bubbling bed reactor. Multiphase Flow 2015. València, Spain2015.

[38] Bruni G, Solimene R, Marzocchella A, Salatino P, Yates JG, Lettieri P, et al. Self-segregation of high-volatile fuel particles during devolatilization in a fluidized bed reactor. Powder Technology. 2002;128:11-21.

[39] Qin K, Thunman H. Diversity of chemical composition and combustion reactivity of various biomass fuels. Fuel. 2015;147:161-9.

[40] Rouquerol J, Avnir D, Everett DH, Fairbridge C, Haynes M, Pernicone N, et al. Guidelines for the Characterization of Porous Solids. Studies in Surface Science and Catalysis1994. p. 1-9.

[41] Niklasson F, Thunman H, Johnsson F, Leckner B. Estimation of solids mixing in a fluidized-bed combustor. Ind Eng Chem Res. 2002;41:4663-73.

[42] Sette E, Aimé, S., Pallarès, D., Johnsson, F. Analysis of lateral fuel mixing in a fluid-dynamically down-scaled bubbling fluidized bed Fluidization XIV. Noordwijkerhout, The Netherlands2013. p. 877-84.

[43] Peng FF, Lee IC, Yang RYK. Reactivities of in situ and ex situ coal chars during gasification in steam at 1000–1400°C. Fuel Processing Technology. 1995;41:233-51.

[44] Lundberg L, Tchoffor, P.A., Johansson, R., Pallarès, D. Determination of Kinetic Parameters for the Gasification of Biomass Char Using a Bubbling Fluidised Bed Reactor. 22nd International Conference on Fluidized Bed Conversion. Turku, Finland2015.